

Dedicated to Full Member of the Russian Academy of Sciences  
B.A. Trofimov on the 65th Anniversary of His Birth

## Quantum-Chemical Study of the Mechanism of Formation of 1- and 2-(Trimethylsilylmethyl)benzotriazoles

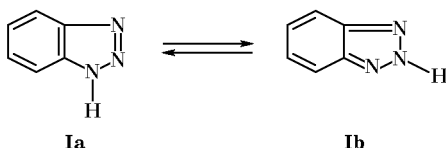
V. A. Shagun, E. I. Brodskaya, O. M. Trofimova, and M. G. Voronkov

Favorskii Irkutsk Institute of Chemistry, Siberian Division, Russian Academy of Sciences,  
ul. Favorskogo 1, Irkutsk, 664033 Russia  
e-mail: omtrof@irioch.irk.ru

Received May 28, 2003

**Abstract**—Quantum-chemical study of the mechanism of formation of 1- and 2-(trimethylsilylmethyl)benzotriazoles, including the reaction of 1,2,3-benzotriazole with sodium methoxide, showed that the predominant formation of the 1-substituted isomer is determined by favorable combination of the thermodynamic and kinetic parameters of the process.

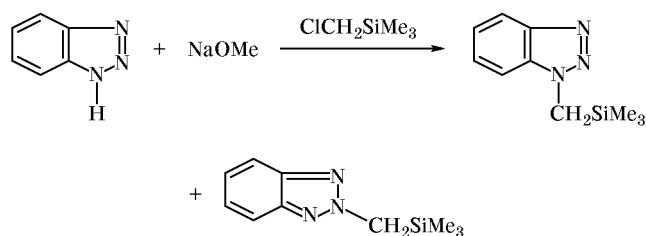
Numerous theoretical and experimental studies have been reported on the relative stability of the benzoid (**Ia**) and *ortho*-quinoid (**Ib**) tautomers of 1,2,3-benzotriazole [1–9].



Quantum-chemical estimations of thermodynamic stability of benzotriazole in the gas phase by various methods give no grounds to believe that one of the above isomers absolutely prevails [4, 7]. According to the experimental data, benzotriazole in crystal and in solution exists mainly in the more polar benzoid form **Ia** [1–7]. As estimated by IR spectroscopy [5], the 1*H*-tautomer is more stable than the 2*H*-tautomer by 5 kJ/mol [5], and the fraction of the latter at 90°C does not exceed 20% [6, 7].

Both 1- and 2-substituted isomers were identified in the thermal isomerization of 1(2)-*R*-benzotriazoles, where *R* = PhCH<sub>2</sub>, Ph<sub>2</sub>CH, Ph<sub>3</sub>C, (4-MeOC<sub>6</sub>H<sub>4</sub>)<sub>2</sub>CH; their ratio depended on the degree of branching of the substituent [10]. We previously found that the reaction of benzotriazole with sodium methoxide yields only sodium 2-benzotriazolide [11]. The latter reacts with chloromethyl(trimethyl)silane to give 1- and 2-(trimethylsilylmethyl)benzotriazoles at a molar ratio of 4:1.

We performed a quantum-chemical study of the mechanism of formation of 1- and 2-substituted benzotriazoles with the goal of elucidating the reasons for complete shift of the equilibrium toward sodium 2-benzotriazolide and for its displacement toward the 1-isomer in the reaction with chloromethyl(trimethyl)silane, as well as of revealing possible differences in the reaction mechanisms.



Nonempirical quantum-chemical calculations were performed at the HF and B3LYP levels with the 6-311G\*\* basis set using GAUSSIAN-98 software [12]. The geometric parameters of molecular systems corresponding to transition structures ( $\lambda = 1$ , where  $\lambda$  is the number of negative Hessian eigenvalues for a given stationary point [13]) and energy minima ( $\lambda = 0$ ) on the potential energy surface (PES) were optimized to a gradient value of  $10^{-5}$  a.u./bohr. In the analysis of planar PES regions, the limiting values were set at about  $10^{-6}$  a.u./bohr. The force constant matrix was calculated analytically using a subprogram incorporated in GAUSSIAN. The structures corre-

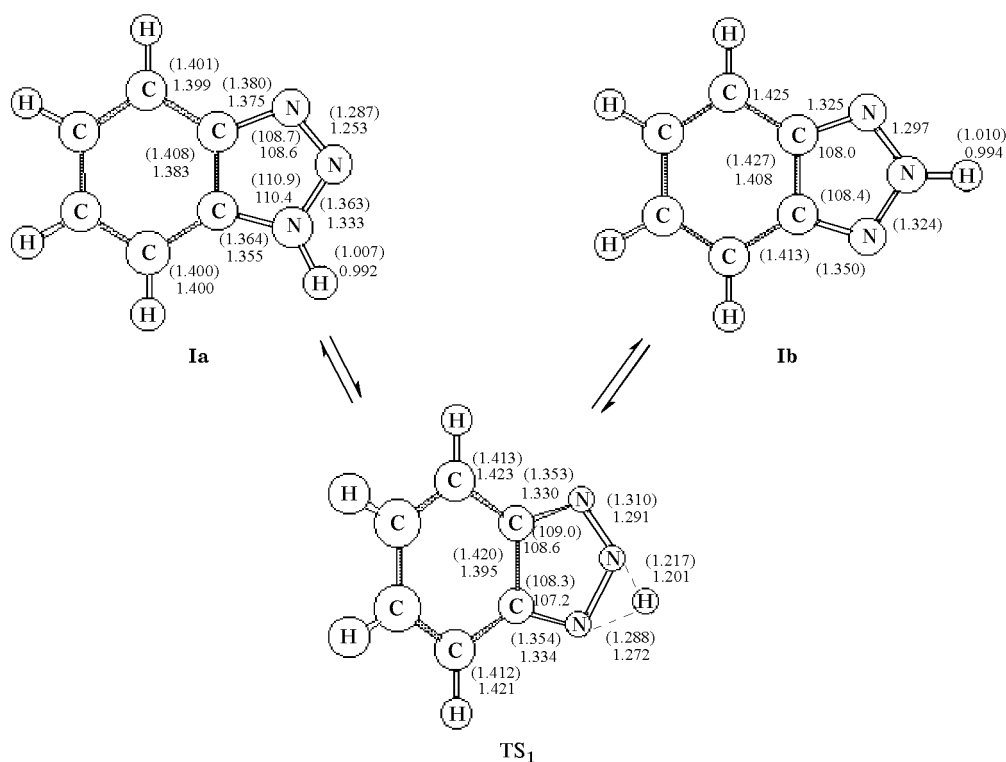


**Fig. 1.** Structures and principal geometric parameters (bond lengths, Å, and bond angles, deg) of stationary states of the benzoid (**Ia**) and *ortho*-quinoid (**Ib**) forms of benzotriazole and of transition state TS<sub>1</sub>, calculated by the HF/6-311G\*\* and B3LYP/6-311G\*\* (in parentheses) methods.

sponding to energy minima on the PES were localized by moving along the gradient line (fastest descend technique) from a saddle point to the nearest critical point. An initial small shift along the transition vector was set to ensure proper determination of the reaction path [13].

The intramolecular prototropic rearrangement of 1*H*-benzotriazole in the gas phase is characterized by a fairly high activation barrier. The 1,2-hydride shift involves a three-membered transition state with a two-electron three-center bond (Fig. 1). The activation energy of the process **Ib** → **Ia** is equal to 258.6 (HF) and 219.9 kJ/mol (B3LYP) with no account taken of zero-point harmonic vibration energy (ZPE). With a correction for ZPE, these values decrease to 242.0 and 201.7 kJ/mol, and the difference in the thermodynamic stability of isomers **Ia** and **Ib** becomes smaller (Table 1). In the transition state (TS<sub>1</sub>), the migrating proton goes out of the five-membered ring plane by 67.7° (64.1°). The transition state configuration is closer to the *ortho*-quinoid structure (Fig. 1).

The formation of prereaction bimolecular complex **IIa** by molecule **Ia** and NaOMe (Fig. 2) gives a considerable gain in energy relative to the isolated components. With no ZPE taken into account, the heat

of complex formation is 123.5 and 166.3 kJ/mol, according to the HF and B3LYP calculations, respectively. With regard to ZPE, these values decrease by 2.4 and 6.5 kJ/mol, respectively. The heat of the exchange reaction **IIa** → **IIIa** is 52.2 (HF) and 43.4 kJ/mol (B3LYP) (Fig. 2). The structure of transition state TS<sub>2</sub> (four-center) suggests that the exchange reaction follows almost synchronous mechanism. Its activation energy is small, 25.3 (HF) and 24.3 kJ/mol (B3LYP). Introduction of a correction for ZPE slightly levels the difference in the thermodynamic stabilities of complexes **IIa** and **IIIa** and reduces the activation barrier by 6.3 and 7.4 kJ/mol, respectively (Table 1).

Analysis of the gradient path connecting initial bimolecular complex **IIb** and product **IIIb** shows that the mechanisms of reactions of NaOMe with isomers **Ia** and **Ib** are different (Fig. 2). The optimal reaction channel does not include synchronous transfer of hydrogen and sodium. It is a two-step ionic process. Initially, proton migrates from the N<sup>2</sup> atom to oxygen through a small barrier ( $\Delta E_a = 4.9$  kJ/mol), yielding an intermediate ionic bimolecular complex, and next follows dissociation of the Na–O bond. Regardless of the mechanism of formation of bimolecular complex

**Table 1.** Total energies ( $E_{\text{tot}}$ ), relative energies ( $\Delta E$ ), numbers of negative Hessian eigenvalues ( $\lambda$ ), energies of zero-point harmonic vibrations (ZPE), imaginary or least harmonic frequencies ( $i\omega/w_1$ ), and electric dipole moments ( $\mu$ ) of structures **Ia** and **Ib**, NaOMe and HOME molecules, bimolecular complexes **IIa**, **IIb**, products **IIIa** and **IIIb**, and transition states TS<sub>1</sub> and TS<sub>2</sub>, calculated by the HF/6-311G\*\* and B3LYP/6-311G\*\* (in parentheses) methods

Structure	$E_{\text{tot}}$ , a.u.	$\Delta E$ , kJ/mol	$\lambda$	ZPE, a.u.	$i\omega/w_1$ , cm <sup>-1</sup>	$\mu$ , D
<b>Ia</b>	-393.50844 (-395.96353)	0 (0.8)	0 (0)	0.11397 (0.10581)	242 (221)	4.01 (3.99)
<b>Ib</b>	-393.50502 (-395.96386)	9.0 (0)	0 (0)	0.11509 (0.10680)	240 (226)	0.22 (0.10)
TS <sub>1</sub>	-393.40642 (-395.88005)	267.6 (219.9)	1 (1)	0.10986 (0.09990)	<i>i</i> 1763 ( <i>i</i> 1727)	3.65 (3.45)
<b>IIa</b>	-669.89785 (-673.49258)	52.2 (43.4)	0 (0)	0.15681 (0.14730)	44 (28)	2.92 (2.81)
<b>IIIa</b>	-669.91776 (-673.49913)	0 (0)	0 (0)	0.15945 (0.14952)	35 (19)	8.09 (7.30)
TS <sub>2</sub>	-669.88821 (-673.48733)	77.5 (67.7)	1 (1)	0.15523 (0.15012)	<i>i</i> 873 ( <i>i</i> 849)	3.41 (3.27)
<b>IIb</b>	-669.89395 (-673.48976)	62.8 (51.4)	0 (0)	0.15756 (0.15265)	41 (36)	2.77 (2.63)
<b>IIIb</b>	-669.91791 (-673.50934)	0 (0)	0 (0)	0.15945 (0.15384)	35 (21)	8.09 (7.87)
TS <sub>3</sub>	-669.88783 (-673.48379)	78.9 (67.0)	1 (1)	0.15611 (0.15132)	<i>i</i> 819 ( <i>i</i> 786)	4.41 (4.35)
MeONa	-276.34232 (-277.46566)	-	0 (0)	0.04194 (0.03902)	128 (92)	7.67 (7.10)
HOME	-115.07581 (-115.75739)	-	0 (0)	0.05485 (0.05112)	344 (333)	1.83 (1.71)

**Table 2.** Total energies ( $E_{\text{tot}}$ ), relative energies ( $\Delta E$ ), numbers of negative Hessian eigenvalues ( $\lambda$ ), energies of zero-point harmonic vibrations (ZPE), imaginary or least harmonic frequencies ( $i\omega/w_1$ ), and electric dipole moments ( $\mu$ ) of NaCl and ClCH<sub>2</sub>SiMe<sub>3</sub> molecules, bimolecular complex **IV**, products **Va** and **Vb**, and transition states TS<sub>3</sub> and TS<sub>4</sub>, calculated by the HF/6-311G\*\* and B3LYP/6-311G\*\* (in parentheses) methods

Structure	$E_{\text{tot}}$ , a.u.	$\Delta E$ , kJ/mol	$\lambda$	ZPE, a.u.	$i\omega/w_1$ , cm <sup>-1</sup>	$\mu$ , D
<b>IV</b>	-1461.23695 (-1466.61662)	129.2 (119.5)	0 (0)	0.24967 (0.23456)	13 (14)	5.68 (5.28)
<b>Va</b>	-1461.28621 (-1466.66220)	0 (0)	0 (0)	0.25114 (0.23628)	17 (19)	11.87 (11.29)
<b>Vb</b>	-1461.28408 (-1466.66000)	5.6 (5.8)	0 (0)	0.25037 (0.23590)	19 (15)	9.16 (8.21)
TS <sub>4</sub>	-1461.23573 (-1466.61291)	132.4 (129.3)	1 (1)	0.24716 (0.23275)	<i>i</i> 2176 ( <i>i</i> 2111)	10.34 (10.11)
TS <sub>5</sub>	-1461.22758 (-1466.60513)	153.8 (149.7)	1 (1)	0.24683 (0.23188)	<i>i</i> 2249 ( <i>i</i> 2195)	10.56 (10.42)
NaCl	-621.43238 (-622.60026)	-	0 (0)	0.00081 (0.00081)	359 (353)	9.53 (9.10)
ClCH <sub>2</sub> SiMe <sub>3</sub>	-906.40363 (-908.88883)	-	0 (0)	0.14698 (0.13907)	71 (65)	2.59 (2.42)

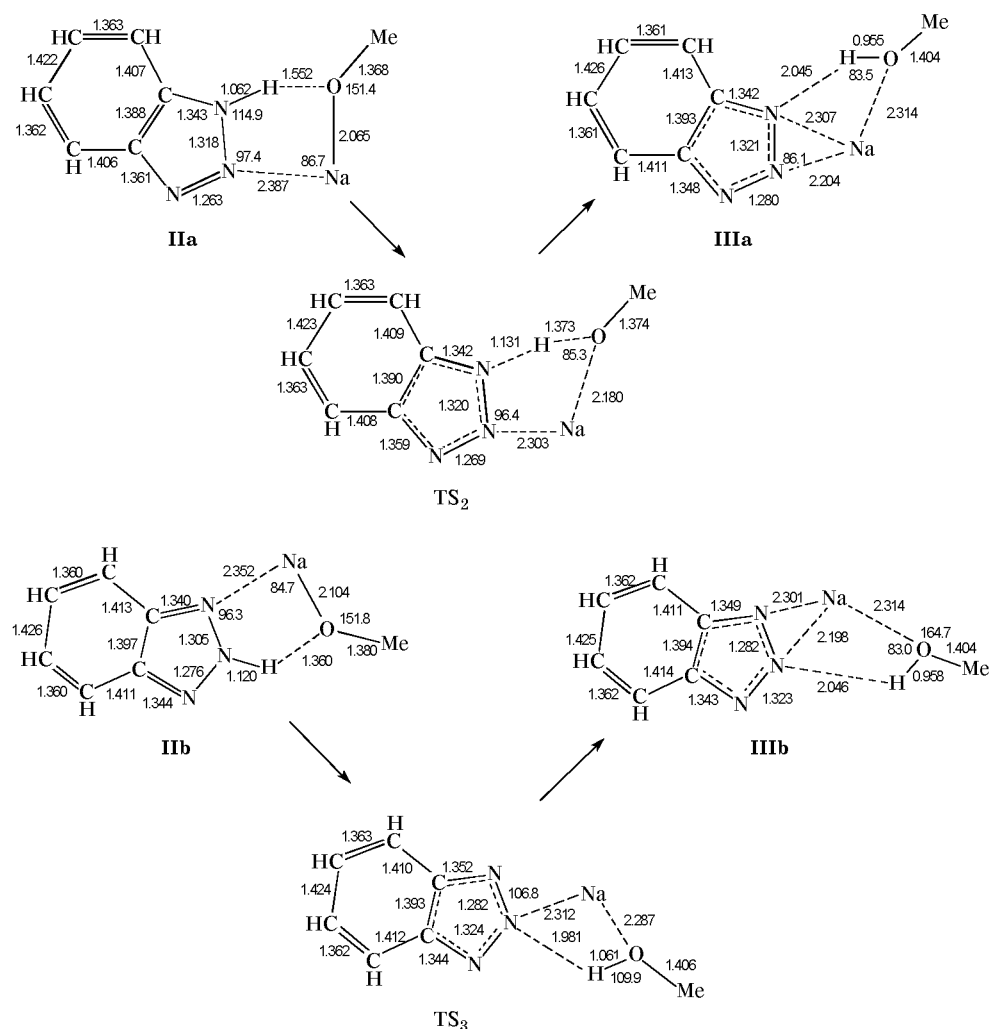


**Fig. 2.** Structures and principal geometric parameters (bond lengths, Å, and bond angles, deg) of bimolecular complexes **IIa** and **IIb**, products **IIIa** and **IIIb**, and transition states **TS<sub>2</sub>** and **TS<sub>3</sub>**, calculated by the HF/6-311G\*\* method.

(**IIIa** or **IIIb**), the  $N^2 \cdots Na$  distance is shorter than  $N^1 \cdots Na$  by 0.1 Å (Fig. 2). This means that the sodium atom in salts **IIIa** and **IIIb** is coordinated mainly to  $N^2$ , in keeping with the experimental data [11].

The different mechanisms of the reactions **IIa** → **IIIa** and **IIb** → **IIIb** are likely to result from the different acidities of tautomers **Ia** and **Ib** which are related to the N–H bond energies. The N–H bond in **Ib** is weaker than in **Ia**, and this is reflected in the tautomer structures. In the gas phase, the N–H bond in molecule **Ib** is longer than in **Ia** (Fig. 1). Presumably, this is the main factor responsible for the two-step character of the transformation **IIb** → **IIIb**. The activation energy in the rate-determining stage is lower (16.1 and 15.7 kJ/mol for HF and B3LYP, respectively) than in the transformation **IIa** → **IIIa**. It is quite probable that, despite approximately similar

thermodynamic stabilities of the tautomers [4, 7], the equilibrium  $Ia + HR \rightleftharpoons Ib + HR$  in protic media shifts toward the 1*H*-tautomer due to different proton exchange mechanisms and hence different activation energies of the direct and reverse processes. This assumption is indirectly proved by the temperature–concentration dependence of the populations of the benzoid and *ortho*-quinoid tautomers [6].

The heat of formation of complex **IV** in the reaction of sodium benzotriazolide with chloromethyl(trimethyl)silane (Fig. 3) is 52.7 (HF) and 54.9 kJ/mol (B3LYP) relative to the isolated components. These values are reduced by 2.8 and 3.0 kJ/mol, respectively, when a correction for ZPE is introduced. The calculated heat of formation of complex **IV** is considerably smaller than those found for complexes **IIa** and **IIIb**. This may be due to the presence of a bulky

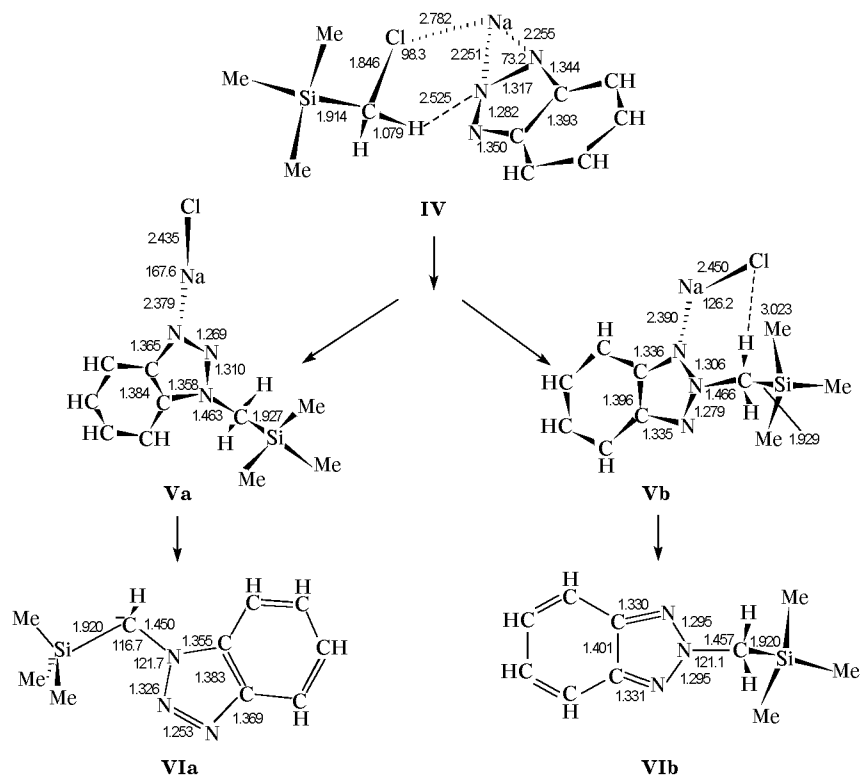


**Fig. 3.** Structures and principal geometric parameters (bond lengths, Å, and bond angles, deg) of bimolecular complex **IV** products **Va** and **Vb**, and isolated molecules **VIa** and **VIb**, calculated by the HF/6-311G\*\* method.

trimethylsilylmethyl group which hampers formation of a tight ion pair with charge transfer.

1- and 2-(Trimethylsilylmethyl)benzotriazoles **Va** and **Vb** (Fig. 3) are thermodynamically more stable than the parent bimolecular complex by 129.2 and 123.6 kJ/mol (HF) and 119.5 and 113.7 kJ/mol (B3LYP), respectively. From the viewpoint of thermodynamics, the formation of the 1-isomer is preferred (Table 2). Analysis of the gradient path connecting complex **IV** and reaction products **Va** and **Vb** suggests the following evolution of the substitution process. Initially, the main contribution to the reaction coordinate for the reaction of chloromethyl(trimethyl)silane with sodium benzotriazolide is that of dissociation of the C–Cl bond and steric reorientation of the sodium atom, which involves change of its coordination mode and choice of one of the triazole nitrogen atom ( $N^1$  or  $N^3$ ) as partner. Then the main constituent of the reaction coordinate changes. The emerging carbocationic center begins to react with lone electron pair of one of the double-bonded nitrogen atoms,  $N^2$  or  $N^3$  ( $N^1$ ). Here, the topologies of the reaction channels leading to 1- and 2-substituted products remain similar up to a branchpoint characterized by the following parameters:  $l(C^+ - N^2) =$

$2.541 \text{ \AA}$ ,  $l(C^+ - N^{3(1)}) = 2.309 \text{ \AA}$ ,  $E_a = 91.7 \text{ kJ/mol}$  (HF calculations). After that point, the reaction channels branch off. The activation energy for formation of the 1-substituted benzotriazole isomer is 132.4 (HF) and 129.3 kJ/mol (B3LYP). The corresponding values for the 2-isomer are 153.8 and 149.7 kJ/mol. The trimethylsilylmethyl group in products **Va** and **Vb** is orthogonal to the benzotriazole ring plane (Fig. 3). However, the most stable structure in the gas phase is that with coplanar arrangement of the heavy atoms, except for the methyl groups (structure **VIa** in Fig. 3). In the isolated molecule of 2-(trimethylsilylmethyl)benzotriazole, orthogonal configuration is the most favorable (structure **VIb** in Fig. 3). Thus, unlike the mechanism found for the reaction of tautomer **Ia** with sodium methoxide, the mechanisms of formation of 1- and 2-(trimethylsilylmethyl)benzotriazoles by reaction of sodium benzotriazolide with chloromethyl(trimethyl)silane are essentially similar. The predominant formation of the 1-isomer (**Va**) is the result of more favorable relation between the thermodynamic and kinetic parameters of the reaction.

This study was financially supported by the Russian Foundation for Basic Research (project no. 01-03-32723).

## REFERENCES

1. Escande, A., Lapasset, J., Faure, R., Vincent, E.-J., and Elguero, J., *Tetrahedron*, 1974, vol. 30, p. 2902.
2. Fischer, G., Cao, X., and Purchase, R.L., *Chem. Phys. Lett.*, 1996, vol. 262, p. 689.
3. Velino, B., Cane, E., Gagliardi, L., Trombetti, A., and Caminati, W., *J. Mol. Spectrosc.*, 1993, vol. 161, p. 136.
4. Negri, F. and Caminati, W., *Chem. Phys. Lett.*, 1996, vol. 260, p. 119.
5. Catalan, J., Perez, P., and Elguero, J., *J. Org. Chem.*, 1993, vol. 58, p. 5276.
6. Tomas, F., Catalan, J., Perez, P., and Elguero, J., *J. Org. Chem.*, 1994, vol. 59, p. 2799.
7. Roth, W., Spangenberg, D., Janzen, Ch., Westhal, A., and Schmitt, M., *Chem. Phys.*, 1999, vol. 248, p. 17.
8. Cane, E., Trombetti, A., and Velino, B., *J. Mol. Spectrosc.*, 1993, vol. 158, p. 399.
9. Kiszka, M., Dunkin, I.R., Gebicki, J., Wang, H., and Wirz, J., *J. Chem. Soc., Perkin Trans. 2*, 2000, p. 2420.
10. Katritzky, A.R., Perumal, S., and Fan, W.Q., *J. Chem. Soc., Perkin Trans. 2*, 1990, p. 2059.
11. Trofimova, O.M., Brodskaya, E.I., Bolgova, Yu.I., Chernov, N.F., and Voronkov, M.G., *Dokl. Ross. Akad. Nauk*, 2003, vol. 388, p. 208.
12. Frisch, M.J., Trucks, G.W., Schlegel, H.B., Scuseria, G.E., Robb, M.A., Cheeseman, J.R., Zakrzewski, V.G., Montgomery, J.A., Stratmann, R.E., Burant, J.C., Dapprich, S., Millam, J.M., Daniels, A.D., Kudin, K.N., Strain, M.C., Farkas, O., Tomasi, J., Barone, V., Cossi, M., Cammi, R., Mennucci, B., Pomelli, C., Adamo, C., Clifford, S., Ochterski, J., Petersson, G.A., Ayala, P.Y., Cui, Q., Morokuma, K., Malick, D.K., Rabuck, A.D., Raghavachari, K., Foresman, J.B., Cioslowski, J., Ortiz, J.V., Stefanov, B.B., Liu, G., Liashenko, A., Piskorz, P., Komaromi, I., Gomperts, R., Martin, R.L., Fox, D.J., Keith, T., Al-Laham, M.A., Peng, C.Y., Nanayakkara, A., Gonzalez, C., Challacombe, M., Gill, P.M.W., Johnson, B., Chen, W., Wong, M.W., Andres, J.L., Gonzalez, C., Head-Gordon, M., Replogle, E.S., and Pople, J.A., *Gaussian 98 (Revision A.6)*, Pittsburgh, PA: Gaussian, 1998.
13. Minyaev, R.N., *Usp. Khim.*, 1994, vol. 63, p. 939.